



## OPEN

# Role of SLC6A6 in promoting the survival and multidrug resistance of colorectal cancer

SUBJECT AREAS:  
COLORECTAL CANCER  
CANCER STEM CELLS  
CANCER THERAPEUTIC RESISTANCE  
APOPTOSIS

Masahiro Yasunaga & Yasuhiro Matsumura

Division of Developmental Therapeutics, Research Center for Innovative Oncology, National Cancer Center Hospital East, 6-5-1 Kashiwanoha, Kashiwa, Chiba 277-8577, Japan.

Received  
7 February 2014

Accepted  
14 April 2014

Published  
30 April 2014

Correspondence and requests for materials should be addressed to Y.M. (yhmatsum@east.ncc.go.jp)

The treatment of colorectal cancer (CRC) might be improved by the identification of a signalling pathway that could be targeted with novel therapeutics. The results of this study indicate that the taurine transporter SLC6A6 is highly expressed in CRC cells compared with normal colonocytes. SLC6A6 knockdown (KD) attenuated cell survival and was accompanied by enhanced drug sensitivity to 5-fluorouracil (5-FU), doxycycline (DOX) and SN-38. Both the population frequency of the side population (SP) cells and their cancer stem cell (CSC)-like properties (such as tumour initiation, differentiation and chemoresistance) were abrogated by SLC6A6-KD. Conversely, SLC6A6 overexpression increased cell survival and the proportion of SP cells, enhancing multidrug resistance (MDR). Additionally, SLC6A6-siRNA treatment enhanced the cytotoxic effects of all 3 drugs, whereas the efficacy of ABCG2-siRNA treatment was limited to its 2 substrate drugs, DOX and SN-38. This study indicates that SLC6A6 plays an important role in the maintenance of CSC characteristics, thus promoting cell survival signalling and chemoresistance. Therefore, SLC6A6 inhibition may be a promising therapeutic strategy for refractory CRC.

Colorectal cancer (CRC) is one of the most common malignancies in the world<sup>1</sup>. Current CRC chemotherapy regimens are associated with patient prognoses that are far from satisfactory, and the identification of a novel signalling pathway that can be robustly targeted in CRC treatment is strongly desired<sup>2</sup>. In the present study, we adopted two unique methods for identifying CRC-specific molecules. First, we obtained pure normal colonocytes from the lavage solution following colonoscopies, without allowing the contamination of the nonepithelial components. We then performed comprehensive expression analyses comparing the isolated normal colonocytes and CRC cell lines. Second, *in situ* hybridisation (ISH) was used to validate the results of the expression analysis, resulting in the identification of CRC-specific molecules (Figure 1a). Finally, we found that the taurine transporter SLC6A6 was highly expressed in the CRC cells. Taurine plays a role in many biological activities, including osmoregulation, membrane stabilisation, antioxidation, bile salt formation and neurotransmission<sup>3,4</sup>. Mouse models have shown that the genetic inactivation of SLC6A6 increases susceptibility to apoptosis in a variety of cell types<sup>5-7</sup>.

In this study, we clarified the prosurvival and anti-apoptotic effects of SLC6A6 in CRC cells. Moreover, we found that SLC6A6 plays an important role in the maintenance of side population (SP) cells and their cancer stem cell (CSC) properties, including enhanced prosurvival activity, tumour initiation and chemoresistance. Our findings may provide novel targets and approaches for the development of new therapies for refractory CRC.

## Results

**Identification of SLC6A6 as a highly expressed gene in colorectal cancer.** In the first screen, we performed a DNA microarray analysis to select genes that were highly expressed in 5 CRC cell lines (SW480, LoVo, DLD1, HT-29 and HCT116), but not in normal colonocytes obtained from 2 healthy volunteers by lavage. In the second screen, a quantitative reverse transcription polymerase chain reaction (qPCR) analysis was used to validate the candidate genes that were highly expressed in CRC cells. ISH was then performed for the final validation. Each of these methods indicated that the taurine transporter SLC6A6 was a CRC-specific cell surface marker (Figure 1a-e).

**Knockdown of SLC6A6 reduces prosurvival activity and increases multidrug sensitivity in CRC cells.** To address the biological role of SLC6A6 in CRC, we knocked down (KD) the gene in DLD1 and HT-29 cells (two of

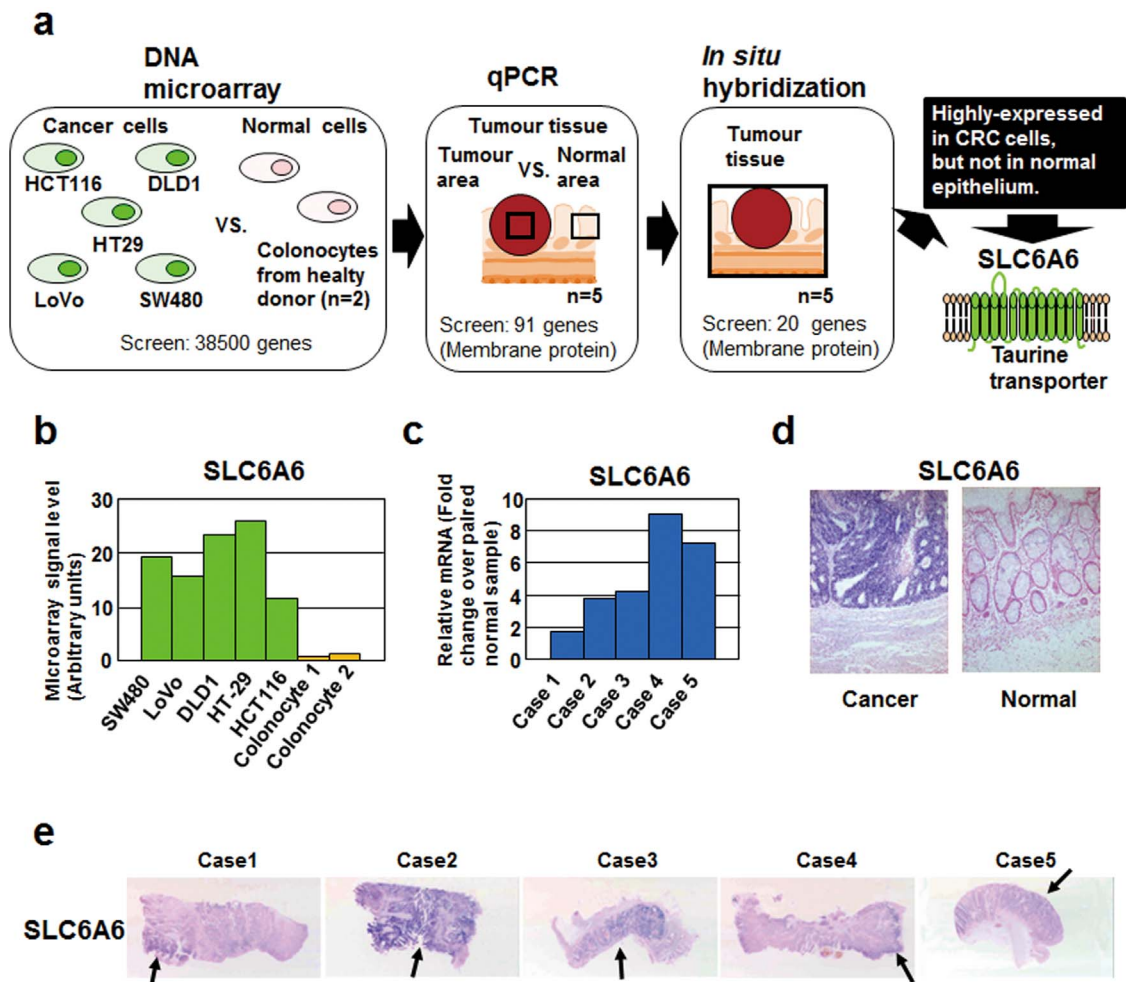


**Figure 1** | Screening strategy and identification of SLC6A6 as a CRC (colorectal cancer)-specific cell surface marker. (a) Schematic outline of the strategy to identify CRC-specific genes. From the microarray results, 91 genes that encode membrane proteins were selected from 38,500 genes in a chip array; from those 91 genes, 20 candidate genes were selected for further study using RT-qPCR. Finally, the taurine transporter SLC6A6, which ISH (*in situ* hybridisation) revealed to be highly expressed in CRC cells but not in corresponding normal epithelial cells, was identified as a CRC-specific cell surface marker. (b) SLC6A6 gene expression in 5 CRC cell lines and 2 colonocyte samples from healthy donors was evaluated using a DNA microarray analysis. (c) SLC6A6 gene expression in 5 clinical samples was evaluated using quantitative RT-PCR. RQ, relative quantification of the tumour-to-normal ratio. (d and e) ISH of SLC6A6 in the clinical samples. Arrow indicates cancer (e).

the cell lines included in the microarray analysis) (Figure 2a). SLC6A6 was also knocked down in HCT-15 cells because they have a higher efficiency SLC6A6-KD than the other initial microarray-analysed cell lines. Taurine uptake was significantly lower in the SLC6A6-KD cells compared with control (GFP-KD) cells (Figure 2b). Taurine is known to support cell growth through the maintenance of osmolality or through membrane protection against various stimuli<sup>3,4</sup>. The growth rate of the SLC6A6-KD cells was also significantly lower than that of the control cells (Figure 2c). However, a cell cycle analysis revealed no clear differences between the SLC6A6-KD cells and the control cells (Figure 2d). Instead, the percentage of annexin V-positive/propidium iodide (PI)-negative apoptotic cells was higher in all of the SLC6A6-KD cell lines (Figure 2e). These data indicate that the SLC6A6 signalling pathway mainly regulates the prosurvival activity of CRC cells.

**SLC6A6 signalling regulates multidrug sensitivity independent of the ABC transporter or 5-FU metabolism.** The sensitivity of the SLC6A6-KD cells to multiple drugs (5-fluorouracil, 5-FU; doxorubicin, DOX; and SN-38 as an active form of camptothecin-11, CPT-11) was between 5- and 100-fold higher than that of the control cells (Figure 3a). The overexpression of ATP-binding cassette (ABC)

transporters, such as MDR1 or ABCG2, is a major cause of multidrug resistance (MDR)<sup>8</sup>. However, the expression of both MDR1 and ABCG2 was preserved in the SLC6A6-KD cells (Figure 3b). We used HCT-15 cells for further evaluations because that cell line exhibited a stronger SLC6A6-KD drug sensitivity phenotype compared with the DLD1 and HT-29 cell lines. Flow cytometry revealed no clear difference in the cellular accumulation of the fluorescent drugs (DOX and CPT-11) between HCT-15 and HCT-15 SLC6A6-KD cells (Figure 3c), which suggests that the ABC transporter remained active in the SLC6A6-KD cells. A cell's sensitivity to 5-FU mainly depends on a metabolic pathway that reduces or abolishes the drug's activity, rather than the ABC transporters<sup>9</sup>. The overexpression of dihydropyrimidine dehydrogenase (DPD) results in 5-FU resistance, whereas the expression of thymidylate synthase (TS) or uridine monophosphate synthetase (UMPS) can increase sensitivity to the drug. Despite an approximately 100-fold increase in sensitivity to 5-FU in the HCT-15 SLC6A6-KD cells, there were no clear differences in TS, UMPS or DPD expression between the HCT-15 SLC6A6-KD cells and the control cells (Figure 3d).

**SLC6A6 signalling is necessary to maintain both the population frequency of side population (SP) cells and their CSC-like properties.**

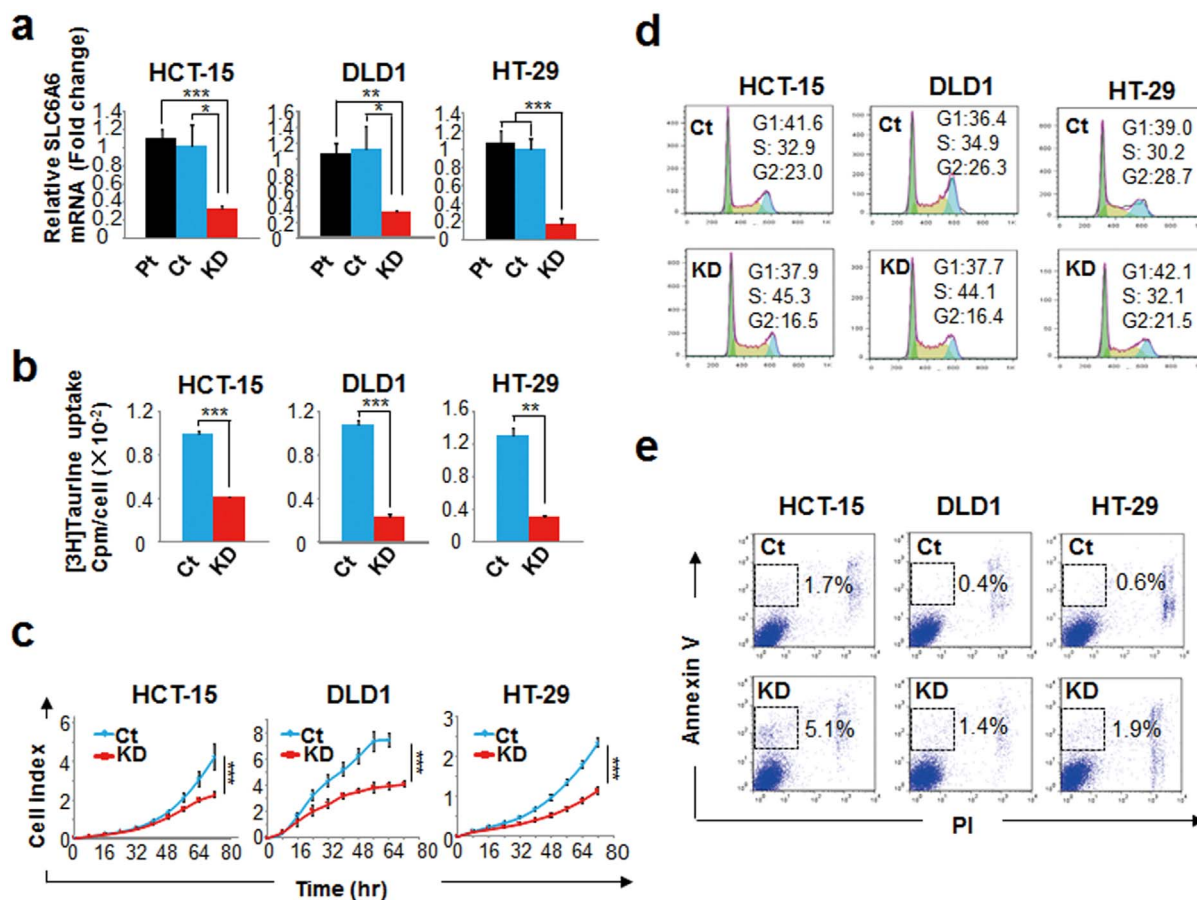


**Figure 2 | SLC6A6 knockdown attenuated pro-survival activity.** (a) Quantitative RT-PCR of SLC6A6 knockdown (KD) in HCT-15-KD, DLD1-KD and HT-29-KD cells compared with the parental cell lines and compared with control (GFP-KD) cells. Each bar represents  $n=3$ ; means  $\pm$  SD. \* $P<0.05$ , \*\* $P<0.01$ , \*\*\* $P<0.001$  (Student's *t*-test). (b) [ $^3$ H]taurine uptake in the SLC6A6-KD and control cells after 50 min incubation. [ $^3$ H] activity was normalised to the cell number in each sample. Each bar represents  $n=3$ ; means  $\pm$  SD. \*\* $P<0.01$ , \*\*\* $P<0.001$  (Student's *t*-test). (c) The cell proliferation kinetics of the SLC6A6-KD and control cells were examined using the xCELLigence system. Each bar represents  $n=3$ ; means  $\pm$  SD. \*\*\* $P<0.001$  (ANOVA). (d) Cell cycle analysis of the SLC6A6-KD and control cells using flow cytometry. The Watson Pragmatic model in the FlowJo Cell Cycle software was used for the analysis. The percentage of G1, S or G2 cells is indicated in each panel. (e) The populations of Annexin V-positive/PI (propidium iodide)-negative apoptotic cells in the SLC6A6-KD and control cells were evaluated using flow cytometry. The percentage of apoptotic cells within the gated regions is indicated in each panel. Pt, parental; Ct, control; KD, knockdown (using short hairpin RNA).

Recent studies of CSCs have indicated that cancer treatment failure is caused by the existence of chemotherapy-resistant CSCs<sup>10</sup>. CSCs might have some anti-apoptotic capabilities, without overexpressing ABC drug transporters or being in a quiescent state<sup>8</sup>. Therefore, we examined whether SLC6A6 signalling affected the CSCs. In all of the SLC6A6-KD cell lines, the numbers of SP cells and CD133<sup>+</sup> cells were substantially decreased, whereas the number of CD44<sup>+</sup> cells remained stable (Figure 4a and Supplementary Figure 1). The levels of LGR5 and ALDH1, which are CSC markers, were also significantly lower in the SLC6A6-KD cell lines (Figure 4b). We then measured the expression of the CRC differentiation markers CEA and KRT20. CEA expression was significantly decreased in all 3 of the SLC6A6-KD cell lines, and KRT20 expression was significantly decreased in the HCT-15 and DLD1 SLC6A6-KD cells (Figure 4c). We also evaluated the chemoresistance of the SP cells. At high doses of 5-FU or DOX, at which most of the SLC6A6-KD cells were not able to survive, the frequency of SP cells in the control CRC cells was between 2- and 10-fold higher than in the untreated controls (Figure 4d). We then evaluated the tumour-initiating activity of the SP cells compared with the remaining SLC6A6-KD and control cells. The SP cells were collected from the HT-29 cells due to the relatively higher proportion of SP cells in the cell line (Figure 4a). In vivo experiments HT-29 cell lines showed that

the frequency of tumour initiation following inoculation with small numbers of SLC6A6-KD SP cells was lower compared with the inoculation of control SP cells (Figure 4e). In particular, there was a significant difference in the tumour size between the inoculations with SLC6A6-KD SP cells and with the control SP cells (Figure 4f).

**Overexpression of SLC6A6 increases the population frequency of SP cells.** To validate the pro-survival role of SLC6A6 in CSCs, we transfected several CRC cell lines with the SLC6A6 gene. The Colo320DM cell line exhibited the highest level of SLC6A6 expression after being transfected. The level of SLC6A6 expression in the SLC6A6-highly expressing (Hi) Colo320DM cells was more than 10-fold higher than that of the parental Colo320DM cell line (Figure 5a); therefore, we used the SLC6A6-Hi Colo320DM cells for further analysis. The SLC6A6-Hi cells exhibited significantly increased taurine uptake compared with the empty vector-transfected controls (Figure 5b). In the early-mid log phase, the growth rates of both cell types were the same. However, in the late log phase, the SLC6A6-Hi cells continued to grow, while the control cells died due to overgrowth or nutrient deficiency (Figure 5c and 5d). Under these conditions, approximately 80% of the control cells died, whereas approximately 90% of the SLC6A6-Hi cells remained

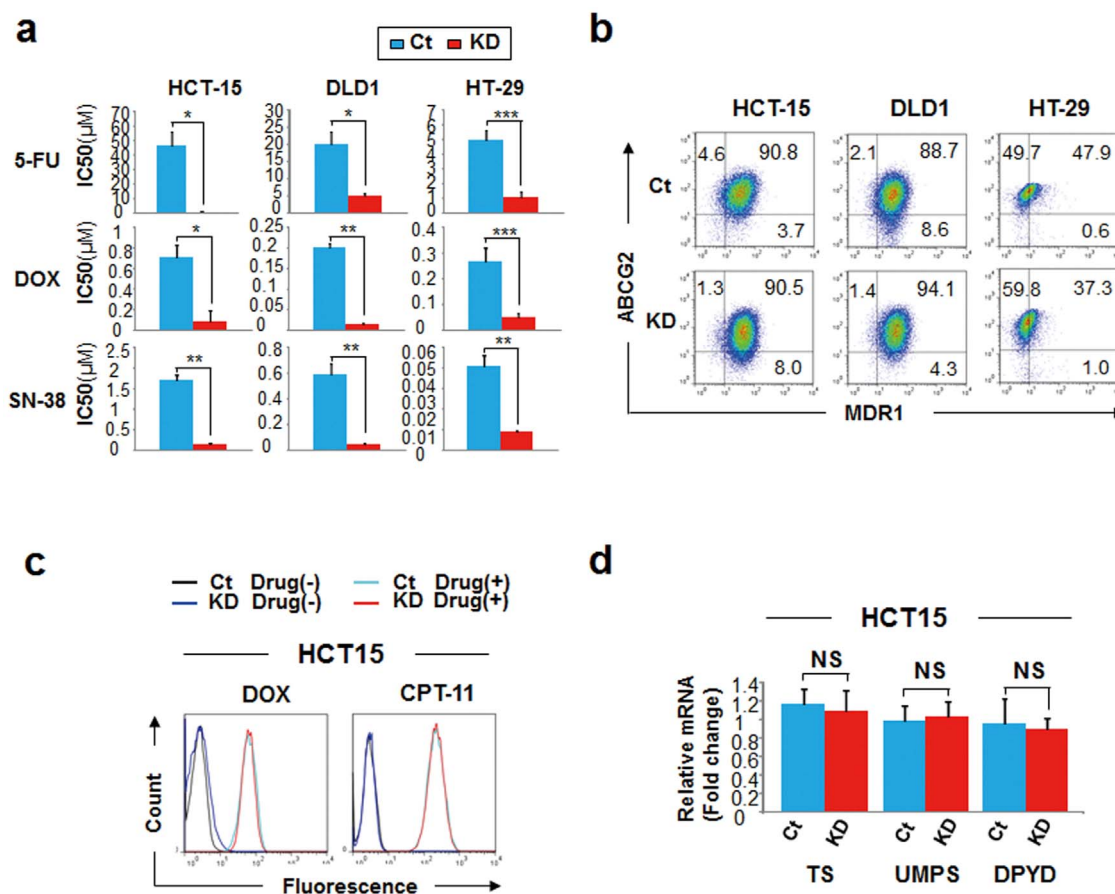


**Figure 3** | SLC6A6 knockdown increases multidrug sensitivity in an ABC transporter- and 5-FU metabolism-independent manner. (a) IC<sub>50</sub> values (μM) of 5-FU, doxorubicin (DOX) or SN-38 of the SLC6A6-KD and control cells. IC<sub>50</sub>, half-maximal inhibitory drug concentration. Each bar represents n=3; means ± SD. \*P<0.05, \*\*P<0.01, \*\*\*P<0.001 (Student's t-test). (b) Estimation of both MDR1 and ABCG2 expression in the SLC6A6-KD and control cells using flow cytometry. The percentage of MDR1-positive/ABCG2-positive cells (upper right), MDR1-negative/ABCG2-positive cells (upper left) and MDR1-positive/ABCG2-negative cells (lower right) is indicated in each panel. (c) The accumulation of the fluorescent drugs 5 hours after treatment with 3 μM DOX or 30 μM CPT-11 (the prodrug of SN-38) in the HCT-15 SLC6A6-KD and control cells was measured using flow cytometry. (d) Quantitative RT-PCR of the molecules involved in 5-FU metabolism in the HCT-15 SLC6A6-KD and control cells. Each bar represents n=3; means ± SD. NS, not significant (Student's t-test). Ct, control; KD, knockdown (using short hairpin RNA).

alive (Figure 5e). In addition, the percentage of SP cells was significantly higher in the SLC6A6-Hi cells (Figure 5f). Furthermore, compared with the control cells, the transcription levels of the CSC markers LGR5 and ALDH1 were significantly higher in the SLC6A6-Hi cells (Figure 5g), and the SLC6A6-Hi cells exhibited significantly lower multidrug sensitivity (Figure 5h). In this experiment, neither CD133 nor CD44 was detected in the control, SLC6A6-Hi or parental Colo320DM cells based on qPCR and flow cytometric analyses (data not shown).

**Differences in the MDR phenotypes and mechanisms of SLC6A6 and ABCG2.** ABCG2, which is a molecular determinant of the SP phenotype, can cause MDR<sup>11,12</sup>. Therefore, we compared the effects of SLC6A6 and ABCG2 on the MDR phenotype. Both SLC6A6 and ABCG2 were expressed on the cell-membrane of HCT-15 CRC cells. However, the merged image revealed that the two molecules were not co-expressed together (Figure 6a). Next, we used siRNA treatment to carry out a functional analysis of the two molecules. Both SLC6A6- and ABCG2-siRNA downregulated their target genes as compared with a nonspecific control siRNA (Figure 6b). Moreover, the cytotoxicity of 5-FU, DOX and SN-38 was enhanced by SLC6A6-siRNA (Figure 6c). ABCG2-siRNA enhanced the cytotoxicity of DOX and SN-38 (its specific substrates), but not the cytotoxicity of 5-FU (Figure 6c). These data strongly indicate that the MDR phenotype of SLC6A6 is quite different from that of ABCG2 with

respect to substrate dependency. It is clear that there are obvious differences between the MDR mechanisms arising from SLC6A6 and ABCG2; the former plays a principal role in cell survival, whereas the latter affects the drug efflux pump.

In addition, publicly available microarray data indicate that patients with high levels of SLC6A6 exhibit significantly shorter disease-free survival times (GEO data set GSE17538, Supplementary Figure 2). Collectively, these data suggest that inhibiting SLC6A6 signalling may improve CRC treatment.

## Discussion

There were several difficulties in identifying and characterising a new target molecule for the diagnosis or treatment of CRC. The comprehensive analysis of gene expression and DNA mutation analysis using DNA microarrays and next-generation sequencing has allowed researchers to easily and quickly identify numerous candidate target molecules<sup>13,14</sup>. However, heterogeneity and the quality of the clinical samples have posed major problems. Clinical samples contain various stromal cells, such as fibroblasts and blood cells, in addition to tumour cells. During storage, transcripts or genomic DNA from surgically excised tissues may be degraded by proteases or ribonucleases in a time- and temperature-dependent manner<sup>15</sup>. However, our comprehensive expression analysis compared CRC cell lines with pure normal colonocytes obtained from colonoscopy lavage solutions without contamination by non-epithelial components. Moreover, our

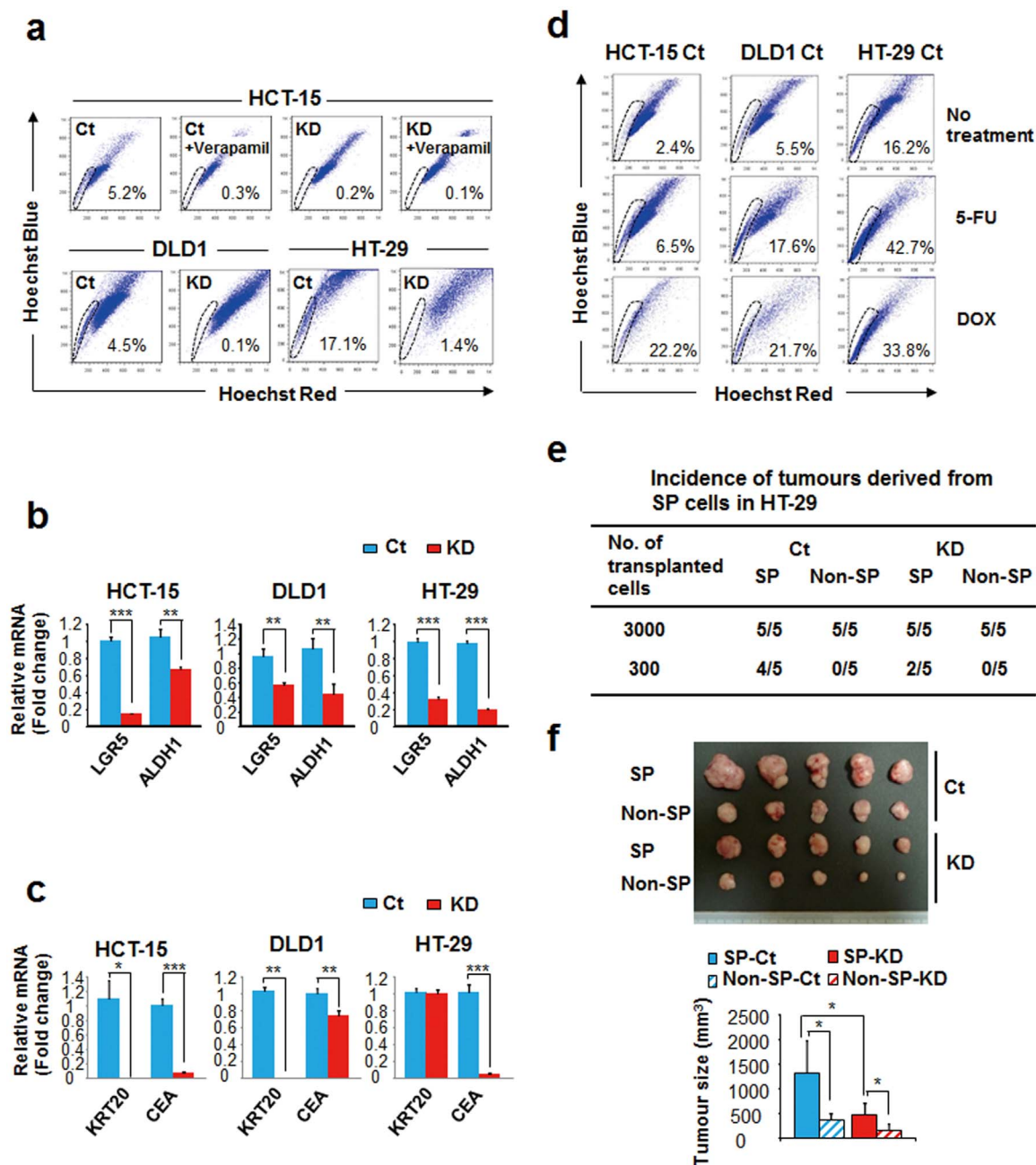


**Figure 4** | Knockdown of SLC6A6 decreases the population frequency of SP cells and attenuates their CSC properties. (a) Flow cytometric analysis of the Hoechst 33342-stained side population (SP) in the SLC6A6-KD and control cells. Verapamil-treated cells were used as a negative control for the SP cells. The percentage of SP cells within the gated regions is indicated in each panel. (b) Quantitative RT-PCR of the CSC markers LGR5 and ALDH1 in the SLC6A6-KD and control cells. Each bar represents  $n=3$ ; means  $\pm$  SD.  $^{**}P<0.01$ ,  $^{***}P<0.001$  (Student's *t*-test). (c) Quantitative RT-PCR of the differentiation markers CK20 and CEA in SLC6A6-KD and control cells. Each bar represents  $n=3$ ; means  $\pm$  SD.  $^{*}P<0.05$ ,  $^{**}P<0.01$ ,  $^{***}P<0.001$  (Student's *t*-test). (d) Frequency changes in the SP cell population after treatment with 5-FU or DOX were analysed using flow cytometry. The cells were exposed to high doses of the drugs (100  $\mu$ M, 30  $\mu$ M and 3  $\mu$ M 5-FU for HCT-15, DLD1 and HT-29, respectively, or 0.3  $\mu$ M, 0.1  $\mu$ M and 0.1  $\mu$ M DOX for HCT-15, DLD1 and HT-29, respectively); these doses were greater than the  $IC_{50}$  value for each SLC6A6-KD cell line. (e) SP cells and non-SP cells were sorted from the HT-29 SLC6A6-KD and control cells using flow cytometry, and their tumour-initiating activity was measured by evaluating the tumour incidence at the implanted sites on nude mice 6 weeks after injection. (f) Tumours were excised and measured 6 weeks after the injection of  $3 \times 10^3$  SP cells or non-SP cells derived from the HT-29 SLC6A6-KD or control cell line. Each bar represents  $n=5$ ; means  $\pm$  SD.  $^{*}P<0.05$  (Student's *t*-test). Ct, control; KD, knockdown (using short hairpin RNA).

validation method, which used ISH on clinical samples, allowed us to identify robust cancer-specific molecules. Thus, we identified the taurine transporter SLC6A6 as a novel CRC-specific gene.

SLC6A6 is a multi-pass membrane protein that transports taurine in a  $Na^{+}$ - and  $Cl^{-}$ -dependent manner. SLC6A6 signalling has also been shown to affect cell proliferation and cell survival<sup>15,17</sup>. Our results

suggest that the reduction in the growth rate of SLC6A6-KD cells was a function of reduced cell survival, rather than reduced cell proliferation regulated by the cell cycle. The overexpression of SLC6A6 enhanced prosurvival activity but did not influence the cell growth rate, which suggests that SLC6A6 signalling plays a major role in cell survival, but not cell proliferation, in CRC cells.

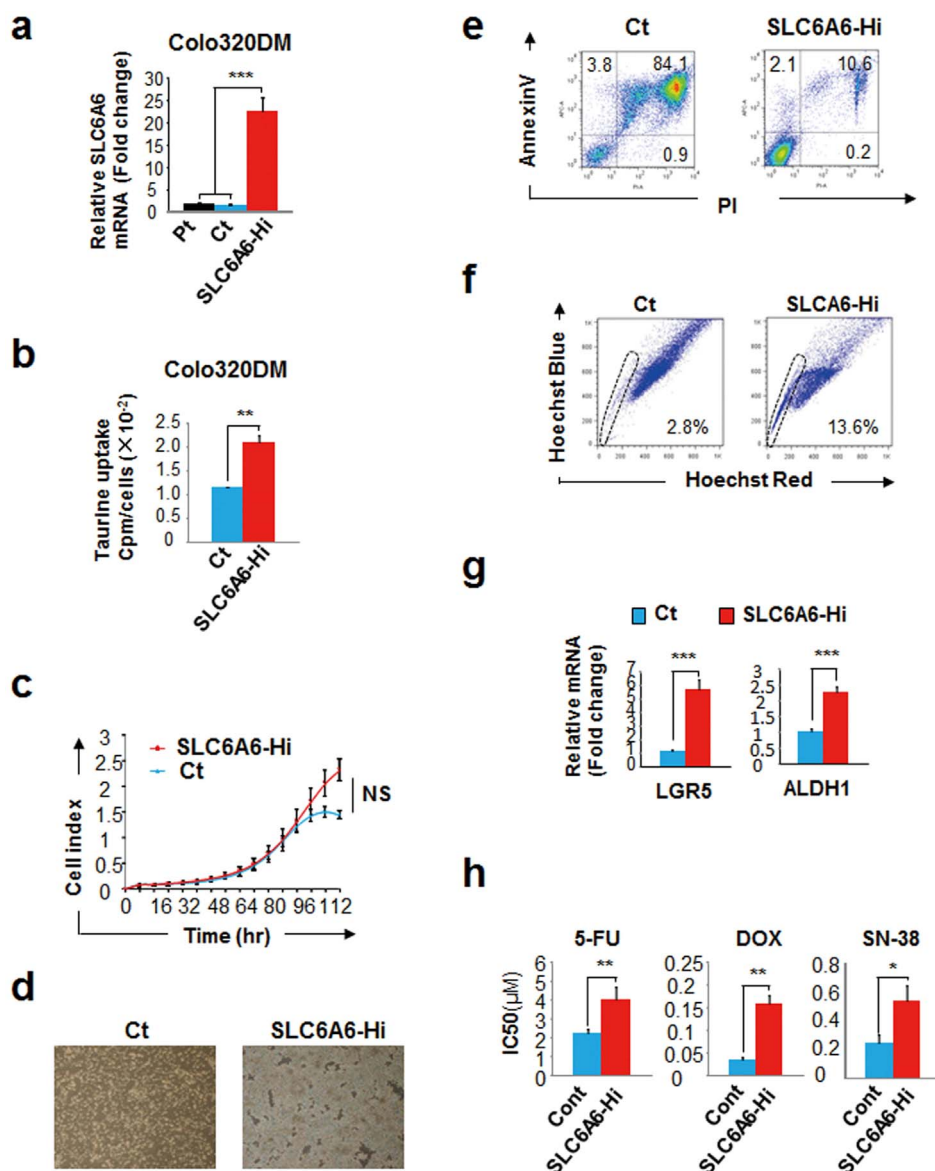


**Figure 5** | Overexpression of SLC6A6 enhances prosurvival activity and increases the frequency of SP cells. (a) Quantitative RT-PCR of SLC6A6 expression in SLC6A6-overexpressing (Hi) Colo320DM cells, empty-vector-transfected cells (controls) and parental cells. Each bar represents  $n=3$ ; means  $\pm$  SD. \*\*\* $P<0.001$  (Student's *t*-test). (b) [ $^3$ H]taurine uptake in SLC6A6-Hi and control cells after incubation for 50 min. Each bar represents  $n=3$ ; means  $\pm$  SD. \*\* $P<0.01$  (Student's *t*-test). (c) The cell proliferation kinetics of SLC6A6-Hi and control cells were examined using the xCELLigence system. Each bar represents  $n=3$ ; means  $\pm$  SD. NS, not significant (ANOVA). (d) Bright-phase images of SLC6A6-Hi and control cells during the late log growth phase (overgrowth state). (e) Flow cytometric analysis of Annexin V-positive/PI-positive dead cells in cultures of SLC6A6-Hi and control cells in the overgrowth state. The percentage of Annexin V-positive/PI-positive dead cells (upper right), Annexin V-positive/PI-negative apoptotic cells (upper left) and Annexin V-negative/PI-positive necrotic cells (lower right) is indicated in each panel. PI, propidium iodide. (f) Flow cytometric analysis of the side populations (SP) of SLC6A6-Hi and control cells. The percentage of SP cells within the gated regions is indicated in each panel. (g) Quantitative RT-PCR of the CSC markers LGR5 and ALDH1 in SLC6A6-Hi and control cells. Each bar represents  $n=3$ ; means  $\pm$  SD. \*\*\* $P<0.001$  (Student's *t*-test). (h) IC<sub>50</sub> value of 5-FU, DOX or SN-38 in SLC6A6-Hi and control cells. IC<sub>50</sub>, half-maximal inhibitory drug concentration. Each bar represents  $n=3$ ; means  $\pm$  SD. \* $P<0.05$ , \*\* $P<0.01$  (Student's *t*-test). Ct, control; SLC6A6-Hi, SLC6A6-overexpressing.

Chemoresistance is one of the most remarkable biological activities associated with SLC6A6 signalling<sup>16,17</sup>. However, the uniqueness of SLC6A6 and its potential crosstalk with other chemoresistance-related proteins, such as the ABC transporter, remain to be determined. Our data demonstrated that SLC6A6 signalling was strongly correlated with MDR (to 5-FU, DOX and SN-38). Although DOX and SN-38 are substrates of the ABC transporter<sup>8</sup>, neither the expression nor the function of the ABC transporters MDR1 and ABCG2 were altered in SLC6A6-KD cells. Moreover, there were no obvious changes in the expression of genes involved in the metabolic pathway shown to inactivate or attenuate 5-FU. Consequently,

the cells were susceptible to chemotherapy-induced apoptosis. In contrast, the SLC6A6-Hi cells were resistant to both apoptosis and chemotherapy, and we believe that both functions were regulated by SLC6A6 signalling.

The CSC hypothesis suggests that tumour cells are heterogeneous and that only the CSC subpopulation has the ability to maintain the capacity to self-renew, proliferate extensively and form new tumours<sup>8,10</sup>. In our study, the number of SP cells, which have a higher survival rate and higher chemoresistance than other cells, was clearly lower in the SLC6A6-KD cells. Moreover, the tumour-initiating activity of the SLC6A6-KD SP cells was lower than in the control

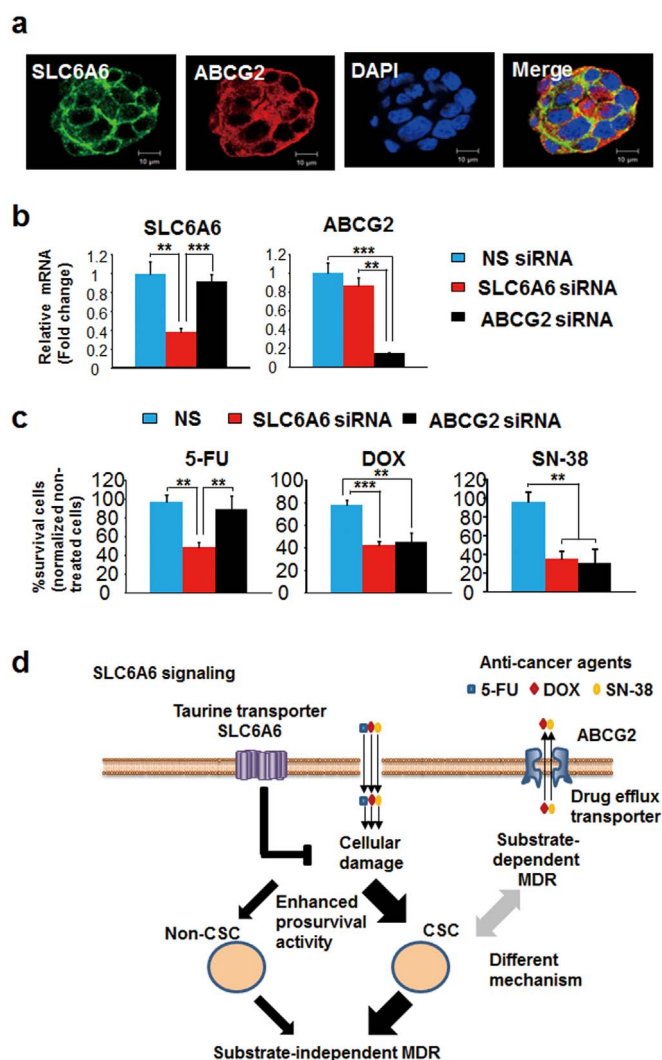


**Figure 6 |** The MDR phenotype and mechanism of taurine-SLC6A6 signalling are different from those of the ABCG2 ABC transporter. (a) SLC6A6 (green), ABCG2 (red) and nuclear (blue) immunostaining of HCT-15 cells. Bar: 10  $\mu$ m. (b) Quantitative RT-PCR of SLC6A6 and ABCG2 in cells treated with nonspecific control-, SLC6A6- or ABCG2-siRNA. NS, nonspecific control. Each bar represents  $n=3$ ; means  $\pm$  SD.  $**P<0.01$ ,  $***P<0.001$  (Student's *t*-test). (c) Drug resistance activity of cells treated with nonspecific control-, SLC6A6- or ABCG2-siRNA. The cells were treated with 3  $\mu$ M 5-FU, 0.1  $\mu$ M doxorubicin (DOX) or 0.01  $\mu$ M SN-38 for 72 h. The percentage of surviving cells was calculated as the ratio of treated to untreated cells. Each bar represents  $n=3$ ; means  $\pm$  SD.  $**P<0.01$ ,  $***P<0.001$  (Student's *t*-test). (d) Schema of model. SLC6A6, which is overexpressed in CRC cells, enhances the pro-survival activity of CRC cells, particularly in highly chemoresistant cancer stem cells (CSCs), thereby promoting multidrug resistance (MDR). This mechanism is quite different from that of the ABCG2-dependent drug-efflux machinery pathway.

SP cells. In contrast, the number of SP cells increased when SLC6A6 was overexpressed, suggesting that SLC6A6 signalling was necessary to maintain both the numbers and CSC properties of the SP cells. SLC6A6-KD also decreased the number of CD133<sup>+</sup> cells, but not the number of CD44<sup>+</sup> cells. However, we were unable to evaluate the expression of CD44 and CD133 in the SLC6A6-Hi cells because these molecules were not expressed in the cells that were originally used as CRC CSC models, including the Colo320DM cell line. The epigenetic inactivation of CD133 in Colo320 cells, a cell line derived from Colo320DM cells, has been reported<sup>18</sup>. Additionally, there have been

reports that CRC possesses both genetic and epigenetic instability, which is manifested by rapid and heterogeneous gene expression patterns<sup>19–21</sup>. Therefore, neither CD44 nor CD133 is a consistent or accurate standard cell surface marker for identifying CSCs. Instead, the MDR phenotype represented by an increase in the number of SP cells may be useful for identifying CSCs irrespective of epigenetic instability.

SP cells can be identified according to their phenotype of reduced Hoechst 33342 accumulation via ABCG2-mediated efflux<sup>11</sup>. Moreover, ABCG2 is also a well-known MDR gene<sup>8</sup>. In mutant mouse analysis, the double knockout of ABCG2 and MDR1 (ABCG2<sup>-/-</sup> MDR1<sup>-/-</sup>) resulted in the complete disappearance of SP cells<sup>12</sup>. However, both the ABCG2<sup>-/-</sup> and ABCG2<sup>-/-</sup> MDR1<sup>-/-</sup> mice were fertile and had normal life spans, indicating that stem cell survival, growth and differentiation were intact. Therefore, the disappearance of the SP cells caused by ABCG2 inhibition reflected a loss of function of the stem cells, but not the disappearance of the stem cells themselves. In the present study, although SLC6A6-KD caused the disappearance of SP cells, the expression and function of both ABCG2 and MDR1 were conserved. We believe that the survival or the maintenance of SP cells as stem cells was difficult due to the low level of SLC6A6 signalling. We also found that the different effects on the MDR phenotype of SLC6A6 and ABCG2 were substrate-dependent. ABCG2 inhibition caused increased sensitivity to its substrates DOX and SN-38 but not to 5-FU, whereas SLC6A6 inhibition caused increased sensitivity to all 3 drugs by attenuating pro-survival activity.

Additionally, the enhancement of pro-survival activity by SLC6A6 signalling resulted in the enrichment of SP cells and the maintenance of their CSC properties, such as tumour initiation. SLC6A6 signalling can enhance MDR activity in both CSC and non-CSC cells. However, we considered that the CSC cells contributed to MDR more than the non-CSC cells because there was a pronounced difference in pro-survival activity between the two cell types. Additionally, SLC6A6 signalling promoted substrate-independent MDR in a manner distinct from the substrate-independent MDR mediated by ABCG2 (Figure 6d). Further investigation is needed to elucidate the detailed mechanism by which SLC6A6 signalling modulates CSC properties. Additional studies should also examine whether SLC6A6 also influences cell survival, drug sensitivity and the proportion of SP cells in other cancers.

In conclusion, our observations strongly suggest that SLC6A6 signalling plays an important role in the survival and maintenance of the CSC population and its capacity for tumour initiation, starvation tolerance and MDR. Therefore, the SLC6A6 pathway may be a promising target for novel anticancer therapeutics to treat refractory CRC.

## Methods

**Cells and cell culture.** The human colon cancer cell lines SW480, LoVo, DLD1, HT-29, HCT116, HCT-15 and Colo320DM were purchased from the American Type Culture Collection (ATCC; Rockville, MD, USA). SLC6A6 gene KD and control cells were established according to our previously reported protocol<sup>22</sup>.

To measure taurine uptake, cells were incubated in a medium containing 0.25  $\mu$ Ci/ml [<sup>3</sup>H]taurine (PerkinElmer, Waltham, MA, USA) for 50 min. The cells were lysed with 0.1 M NaOH and were transferred to scintillation vials. A liquid scintillation cocktail (ULTRA GOLD™, PerkinElmer) was added to the samples, and [<sup>3</sup>H] activity was measured using the Tri-Carb 3110TR liquid scintillation analyser (PerkinElmer). The [<sup>3</sup>H] activity was normalised to the cell number of each sample.

Human exfoliated colonocytes in saline mucosal wash fluid were obtained from two healthy donors during colonoscopy examinations. The cell purification and processing methods were performed as previously described<sup>23</sup>. The experimental protocols and procedures were approved by the institutional review board of the National Cancer Center, Japan.

**DNA microarray and real-time quantitative RT-PCR.** The DNA microarray analysis was performed using 10  $\mu$ g of total RNA from colon cancer cells or exfoliated colonocytes with Affymetrix GeneChip Human Genome U133 plus 2.0 arrays (Santa Clara, CA, USA); the analysis was performed according to standard Affymetrix protocols<sup>24</sup>. From the microarray results, 91 genes that encode membrane proteins,



and which were highly expressed in CRC cells but not in colonocytes from healthy donors, were selected from the 38,500 genes analysed in the chip array (Figure 1a).

The clinical analysis of human CRC was performed by downloading the raw data (CEL files) from a data set (GEO GSE17538) based on 238 samples derived from 177 MCC patients and 61 VMC patients. The data were normalised using the RMA procedure according to previous reports<sup>25–27</sup>. The identification of the probe and annotation were performed using NetAffx, GEO and PubMed. Data from patients with stage 1, 2 or 3 (n=176) tumours were stratified into low and high groups based on the average SLC6A6 expression level.

RNA extraction and RT-qPCR were performed as previously described<sup>23</sup>. Twenty genes that were highly-expressed in CRC tissue compared with paired normal colorectal epithelium were selected for further study (Figure 1a).

**In situ hybridisation.** ISH was performed on the 20 genes that had been selected using RT-qPCR. Based on the ISH results, the taurine transporter SLC6A6, which was highly-expressed in CRC cells but not in the corresponding normal epithelium, was selected for analysis (Figure 1a) using the method described below.

Deparaffinised sections of human tissue (Genostaff Co., Ltd., Tokyo, Japan) were fixed in 4% paraformaldehyde. After treatment with 7 µg/ml proteinase K (Roche, Basel, Switzerland), the sections were refixed in 4% paraformaldehyde and acetylated with 0.25% acetic anhydride. After dehydration, hybridisation was performed using digoxigenin-labelled RNA probes (418 bp fragment of SLC6A6, GenBank accession number NM\_003043, nucleotide positions 5461–5878). After washing, RNase treatment was performed. After rewashing, the sections were treated with a 0.5% blocking reagent (Roche), followed by treatment with 20% heat-inactivated sheep serum (Sigma). After incubation with an alkaline phosphatase (AP)-conjugated anti-DIG antibody (Roche) for 2 h, the sections were visualised using an NBT/BCIP solution (Roche).

**FACS analysis and cell sorting.** FACS analysis and cell sorting were performed as previously described<sup>24</sup>.

*In vitro* cultured cells were stained with PE- or PE-Cy7-anti-CD44 mAb (eBioscience, San Diego, CA, USA), PE- or APC-CD133 mAb (Miltenyi Biotec, Bergisch Gladbach, Germany), Alexa-647 (Life Technologies)-labelled anti-MDR1 (MAB4162, Millipore, MA, USA), biotin-anti-ABCG2 (eBioscience), Alexa-647-labelled annexin V (BioLegend, San Diego, CA, USA) and SA-PE (eBioscience) or SA-PE-Cy7 (BioLegend).

To detect SP cells, dissociated cells were resuspended in DMEM supplemented with 2% foetal calf serum (FCS) and were labelled with 5 to 10 µg/ml Hoechst 33342 (Life Technologies) either with or without 10–30 µg/ml verapamil (Sigma) for 60–90 min at 37°C. The stained cells were analysed using a FACS Calibur or Aria flow cytometer (BD Biosciences). Dead cells, which were stained using propidium iodide (PI) (Life Technologies), were excluded from the analysis.

For the cell cycle analysis, cells fixed in cold 70% ethanol were incubated with a 2.5 µg/ml PI solution containing 0.5 mg/ml RNase (Life Technologies). These cells were then evaluated with a FACS Aria flow cytometer. For the cellular drug accumulation assay, the cells were incubated for 5 h with 3 µM DOX or 30 µM CPT-11. Data were recorded using CellQuest Pro software or BD FACSDiva™ software (BD Biosciences) and were analysed using the FlowJo program (Tree Star, Ashland, OR, USA). The Watson Pragmatic model in the FlowJo Cell Cycle was used for the cell cycle analysis.

**In vitro cell cytotoxicity assay.** The cells were treated with each drug for 72 h, and cytotoxicity was evaluated using the WST-8 assay (Cell Counting Kit-8, Dojindo, Kumamoto, Japan). The reaction signals were evaluated by measuring the absorbance at 450 nm using a microplate reader (SpectraMax 190, Molecular Devices Corp., Sunnyvale, CA, USA).

**Cell growth assay.** Cell growth was quantitatively evaluated in real time using the xCELLigence System (Roche Diagnostics, Mannheim, Germany). The data were analysed with RTCA software (version 1.2, Roche Diagnostics).

**Animal model and tumour-initiating activity.** Female BALB/c nude mice (5 weeks old) were purchased from SLC Japan (Shizuoka, Japan). To evaluate tumour-initiating activity, FACS-sorted cells were resuspended in 50 µl of Opti-MEM I (Life Technologies) and 50 µl of Growth Factor Reduced Matrigel Matrix (BD Biosciences). The mice were inoculated subcutaneously in the flank with  $3 \times 10^2$  or  $3 \times 10^5$  cells. All the animal procedures were performed in compliance with the Guidelines for the Care and Use of Experimental Animals established by the Committee for Animal Experiments of the National Cancer Center. These guidelines meet the ethical standards required by law and also comply with the guidelines for the use of experimental animals in Japan.

**Immunohistochemistry.** Immunostaining was performed as previously described<sup>28</sup>. Anti-SLC6A6 (Atlas Antibodies, Stockholm, Sweden), anti-ABCG2 (Acris Antibodies GmbH, Herford, Germany), Alexa-488- or Alexa-555-labelled anti-mouse IgG (Life Technologies) and Alexa-647-labelled anti-rabbit IgG (Life Technologies) were used. The nuclei were visualised using DAPI staining (Life Technologies). Images were obtained using the LSM 710 Laser Scanning Microscopic system (Carl Zeiss, Oberkochen, Germany) or the BZ-9000 digital high-definition microscopic system (Keyence Co., Osaka, Japan).

**Statistical analysis.** Significant differences between groups were determined using Student's t-test for comparisons of the results from the RT-qPCR of SLC6A6 (Figure 2a, 5a and 6b) or other genes (Figure 3d, 4b, 4c, 5g and 6b), taurine uptake measurements (Figure 2b and 5b), drug sensitivity (Figure 3a, 5h and 6c) and tumour size (Figure 4f). An ANOVA was used to compare cell growth (Figure 2c and 5c), and the log-rank test was used to compare Kaplan-Meier curves (Supplementary Figure 2). All the analyses were performed using SPSS software version 20 (IBM, Armonk, NY, USA).

- Siegel, R., Naishadham, D. & Jemal, A. Cancer statistics, 2013. *CA Cancer J Clin.* **63**, 11–30 (2013).
- Cersosimo, R. J. Management of advanced colorectal cancer, Part 2. *Am J Health Syst Pharm.* **70**, 491–506 (2013).
- Lambert, I. H. Regulation of the cellular content of the organic osmolyte taurine in mammalian cells. *Neurochem Res.* **29**, 27–63 (2004).
- Han, X., Patters, A. B., Jones, D. P., Zelikovic, I. & Chesney, R. W. The taurine transporter: mechanisms of regulation. *Acta Physiol (Oxf).* **187**, 61–73 (2006).
- Warskulat, U. *et al.* Phenotype of the taurine transporter knockout mouse. *Methods Enzymol.* **428**, 439–58 (2007).
- Ito, T. *et al.* Taurine depletion caused by knocking out the taurine transporter gene leads to cardiomyopathy with cardiac atrophy. *J Mol Cell Cardiol.* **44**, 927–37 (2008).
- Kaesler, S. *et al.* Effective T-cell recall responses require the taurine transporter Taut. *Eur J Immunol.* **42**, 831–41 (2012).
- Dean, M., Fojo, T. & Bates, S. Tumour stem cells and drug resistance. *Nat Rev Cancer.* **5**, 275–84 (2005).
- Longley, D. B., Harkin, D. P. & Johnston, P. G. 5-fluorouracil: mechanism of action and clinical strategies. *Nat Rev Cancer.* **3**, 330–8 (2003).
- Jordan, C. T., Guzman, M. L. & Noble, M. Cancer stem cells. *N Engl J Med.* **355**, 1253–61 (355).
- Zhou, S. *et al.* The ABC transporter Bcrp1/ABCG2 is expressed in a wide variety of stem cells and is a molecular determinant of the side-population phenotype. *Nat Med.* **7**, 1028–34 (2001).
- Jonker, J. W. *et al.* Contribution of the ABC transporters Bcrp1 and Mdr1a/1b to the side population phenotype in mammary gland and bone marrow of mice. *Stem Cells.* **23**, 1059–65 (2005).
- Blencowe, B. J. Alternative splicing: new insights from global analyses. *Cell.* **126**, 37–47 (2006).
- Hawkins, R. D., Hon, G. C. & Ren, B. Next-generation genomics: an integrative approach. *Nat Rev Genet.* **11**, 476–86 (2010).
- Haller, A. C. *et al.* Transcriptional profiling of degraded RNA in cryopreserved and fixed tissue samples obtained at autopsy. *BMC Clin Pathol.* **6**, 9 (2006).
- Wersinger, C., Rebel, G. & Lelong-Rebel, I. H. Detailed study of the different taurine uptake system of colon LoVo MDR and non-MDR cell lines. *Amino Acids.* **19**, 667–85 (2000).
- Tastesen, H. S. *et al.* Pinpointing differences in cisplatin-induced apoptosis in adherent and non-adherent cancer cells. *Cell Physiol Biochem.* **26**, 809–20 (2010).
- Yi, J. M. *et al.* Abnormal DNA methylation of CD133 in colorectal and glioblastoma tumors. *Cancer Res.* **68**, 8094–103 (2008).
- Jones, P. A. *et al.* The epigenomics of cancer. *Cell.* **128**, 683–92 (2007).
- Grady, W. M. & Carethers, J. M. Genomic and epigenetic instability in colorectal cancer pathogenesis. *Gastroenterology.* **135**, 1079–99 (2008).
- Gupta, P. B., Chaffer, C. L. & Weinberg, R. A. Cancer stem cells: mirage or reality? *Nat Med.* **15**, 1010–2 (2009).
- Saito, Y. *et al.* The inhibition of pancreatic cancer invasion-metastasis cascade in both cellular signal and blood coagulation cascade of tissue factor by its neutralisation antibody. *Eur J Cancer.* **47**, 2230–9 (2011).
- Koga, Y. *et al.* Detection of colorectal cancer cells from feces using quantitative real-time RT-PCR for colorectal cancer diagnosis. *Cancer Sci.* **99**, 1977–83 (2008).
- Yasunaga, M. *et al.* Induction and monitoring of definitive and visceral endoderm differentiation of mouse ES cells. *Nat Biotechnol.* **23**, 1542–50 (2005).
- Irizarry, R. A. *et al.* Exploration, normalization, and summaries of high density oligonucleotide array probe level data. *Biostatistics.* **4**, 249–64 (2003).
- Dai, M. *et al.* Evolving gene/transcript definitions significantly alter the interpretation of GeneChip data. *Nucleic Acids Res.* **33**, e175 (2005).
- Gentleman, R. C. *et al.* Bioconductor: open software development for computational biology and bioinformatics. *Genome Biol.* **5**, R80 (2004).
- Yasunaga, M., Manabe, S., Tarin, D. & Matsumura, Y. Tailored immunocjugate therapy depending on a quality of tumor stroma. *Cancer Sci.* **104**, 231–7 (2013).

## Acknowledgments

This work was supported by the Funding Program for World-Leading Innovative R&D on Science and Technology (FIRST Program) (YM), the Third Term Comprehensive Control Research for Cancer from the Ministry of Health, Labor and Welfare of Japan (YM), the National Cancer Center Research and Development Fund (YM, MY), and a Grant-in-Aid for Scientific Research from the Japan Society for the Promotion of Science (MY). We would like to thank Dr. T. Sugino for his helpful discussions. We would also like to thank Ms. M. Takigahira, Mrs. M. Araake-Mizoguchi, Mr. Obonai and Mr. Fuchigami for their technical assistance and Mrs. K. Shiina for her secretarial support.





## Author contributions

M.Y. and Y.M. provided the original concept for the research and designed the study. M.Y. performed the experiments. M.Y. and Y.M. discussed the results and wrote the paper.

## Additional information

Supplementary information accompanies this paper at <http://www.nature.com/scientificreports>

**Competing financial interests:** The authors declare no competing financial interests.

**How to cite this article:** Yasunaga, M. & Matsumura, Y. Role of SLC6A6 in promoting the survival and multidrug resistance of colorectal cancer. *Sci. Rep.* **4**, 4852; DOI:10.1038/srep04852 (2014).



This work is licensed under a Creative Commons Attribution-NonCommercial-NoDerivs 3.0 Unported License. The images in this article are included in the article's Creative Commons license, unless indicated otherwise in the image credit; if the image is not included under the Creative Commons license, users will need to obtain permission from the license holder in order to reproduce the image. To view a copy of this license, visit <http://creativecommons.org/licenses/by-nc-nd/3.0/>